Meniscus arrest dominated imbibition front roughening in porous media with elongated pores

2015 J. Phys.: Conf. Ser. 638 012007

(http://iopscience.iop.org/1742-6596/638/1/012007)

Journal of Physics: Conference Series **638** (2015) 012007 doi:10.1088/1742-6596/638/1/012007

Meniscus arrest dominated imbibition front roughening in porous media with elongated pores

Heiko Rieger, Christian Thome and Zeinab Sadjadi

Theoretical Physics, Saarland University, D-66123 Saarbrücken, Germany

E-mail: h.rieger@physik.uni-saarland.de

Abstract. During spontaneous imbibition, a wetting liquid is drawn into a porous medium by capillary forces. Recently, anomalous scaling properties of front broadening during spontaneous imbibition of water in Vycor glass, a nanoporous medium, were reported. The mean height and the width of the propagating front increase with time t both proportional to $t^{1/2}$. We argue that this anomalously large roughening exponent of $\beta = 1/2$ is due to long-lasting meniscus arrests, when at pore junctions the meniscus propagation in one or more branches comes to a halt when the Laplace pressure of the meniscus exceeds the hydrostatic pressure within the junction. From this hypothesis we derive the scaling relations for the emerging arrest time distribution in random pore networks and show that the average front width is proportional to the height yielding a roughness exponent of exactly $\beta = 1/2$ as measured in the Vycor glass imbibition experiments. Extensive simulations of a random pore network model confirm these predictions. Finally, using a microfluidic setup as well as molecular dynamics simulations on the nanoscale, the basic hypothesis of the scaling theory is confirmed by demonstrating the existence of arrest events in Y-shaped junctions, analyzing them quantitatively and comparing them with the theoretical predictions.

1. Introduction

Fluid flow through porous media has been a topic of considerable interest due to its scientific importance and practical applications [1, 2, 3]. Imbibition, which is the displacement of one fluid by another immiscible fluid in a porous matrix, is observable in many everyday processes, for instance when dipping a sugar cube into coffee or dropping ink on a paper. It is important in nature (e.g., for water to flow through soil or to reach all parts of plants) and plays a fundamental role in various industrial areas, ranging from paper and textile treatment to oil recovery and groundwater hydrology [1, 3, 4]. Various physical aspects are involved in the process which makes it an interesting and complex phenomenon, e.g. capillarity, viscous drag, surface tension, hydrostatic pressure, and the quenched disorder of the matrix resulting in random permeability and random capillary pressure.

During imbibition the liquid-gas interface advances and broadens. The time evolution of the invading front follows simple scaling laws, which are independent of the micro- structure and the details of the fluid [5, 6, 7, 8, 9], reminiscent of the universality of critical phenomena. The often complex topology of the porous matrix induces local fluctuations in capillary pressures at the interface as well as hydraulic permeabilities in the bulk. Despite these complexities, the average position of the front $\langle h(t) \rangle$ during a purely spontaneous imbibition evolves as $\langle h(t) \rangle \propto t^{1/2}$,

known as Lucas-Washburn law [11, 12]. This scaling behavior is valid down to nanoscopic pore scales [13, 14, 15].

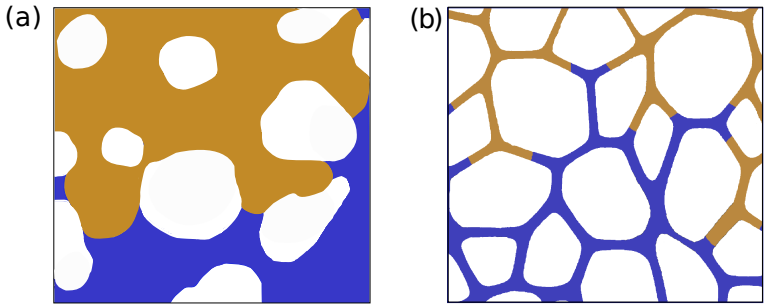

Figure 1. Schematic shape of the imbibition front in a porous structure consisting of (a) small and (b) large aspect ratio pores leading to a continuous liquid gas interface in (a) and isolated mensici in (b).

In most porous materials such as paper and sand, the propagating imbibition front forms a single connected interface between the propagating and the displaced liquid [16], as sketched in Fig. 1a. In these systems, pore space is laterally highly interconnected, resulting in a continuous liquid-gas interface, whose advancement is spatially correlated due to an effective surface tension [17]. Consequently, interface advancement beyond the average front position is slowed down while parts of the interface lagging behind are drawn forward. Hence, the roughening of the interface is reduced and gives rise to dynamical roughening behavior described by universal scaling laws [5, 6, 7, 8, 9].

For pore networks, in which the porous space forms a three-dimensional random network of interconnected pipes with a sufficiently large aspect ratio (ratio between pipe length and radius), the interface between the propagating and the displaced liquid is disconnected and consists of many isolated menisci [2, 18], see Fig.1b for a sketch. The characteristics of the imbibition dynamics of the ensemble of menisci in such pore networks can be expected to be very different from the propagation of continuous interfaces in random media.

Indeed, recent experiments on nanoporous Vycor glass (NVG) showed an anomalously fast front broadening and the absence of a growing correlation length [20]. In this paper we review the experimental situation and our current understanding of the dynamical process in these pore networks with elongated pores. The paper is organized as follows: In section 2 we summarize the experimental results on NVG, in section 3 we discuss the scaling theory for dynamical front broadening based on meniscus arrests at asymmetric pore junctions, section 4 presents the results of computer simulations of a microscopic pore network model involving the hypothesized meniscus arrests, and section 5 discusses experimental evidence for the meniscus arrests at asymmetric pore junctions.

2. Spontaneous imbibition in nano-porous Vycor glass NVG

In [20] the spontaneous imbibition of water into nanoporous Vycor glass (NVG), which is a silica substrate with an interconnected network of nanometer-sized, elongated pores [18] as sketched in Fig. 2a, was investigated. The narrow pores lead to capillary pressures of several hundred times atmospheric pressure. This means that gravity would only halt capillary rise after several kilometers and several billion years [21]. Hence, with this system, one is able to observe pure spontaneous imbibition over large length (centimeter) and long time (hours) scales. The observation of the advancing front is difficult since it is deeply buried inside the matrix, but neutron radiography allowed to image the liquid inside the porous material.

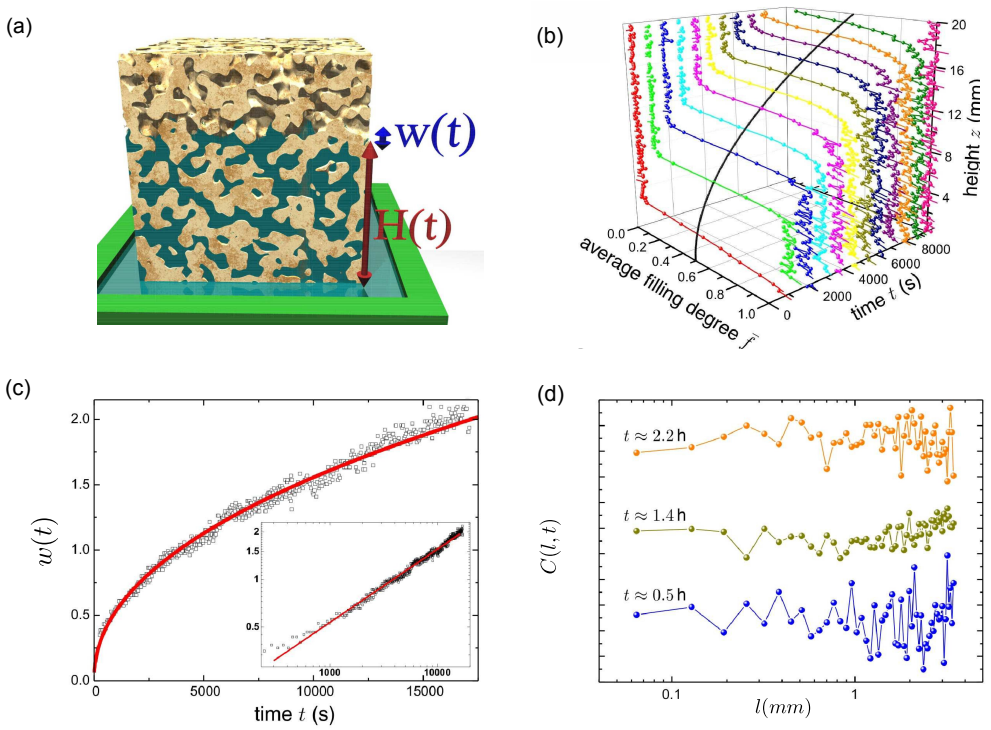

Figure 2. **Spontaneous imbibition in NVG – experimental results** (from [20])**:** a) Schematic representation of spontaneous imbibition of a fluid into a porous matrix like NVG. The arrows indicate the average rise level H(t) and the invasion front width w(t). b) Laterally averaged filling degree $\overline{f}(z,t)$ as a function of height z and time t. The Lucas-Washburn law $z \propto t^{1/2}$ is shown as solid line. c) Evolution of the front width w(t) along with a fit of $w \propto t^{\beta}$ (solid line). The inset shows the same data in a log-log representation. d) Height-height correlation function $C(l,t)$ of the invasion front at three different times, the data are shifted for clarity.

From neutron images [20] the spatial and temporal evolution of the local filling degree $0 \leq f(x,z,t) \leq 1$ are determined. Due to the projection in the y-direction, this is the average amount of filled pore space at lateral position x, height z and time t. Its lateral average, that is the vertical concentration profile $\bar{f}(z,t) \equiv \langle f(x,z,t)\rangle_{\mathrm{x}}$, is shown in Fig. 2b. The time-dependence of the front height, quantified by the mean median rise level $H(t) \equiv \langle z(f{=}0.5,x,t)\rangle_{\mathrm{x}}$, follows the Lucas-Washburn $\sqrt{t}$-law (Fig. 2b, solid lines). Fits of Gauss error functions to the profiles yield the time-dependence of the width $w(t)$ (Fig. 2c). The fit of $w(t) \propto t^{\beta}$ results in a growth exponent of the width or roughness, $\beta = 0.46 \pm 0.01$ (Fig. 2c, solid line). The value $\beta = 0.46$ significantly exceeds previous theoretical predictions, in particular those from phase-field models which are based on quenched, random fields. Such models predict slower roughening dynamics with $\beta \approx 0.19$ and a strong spatial correlation of the height fluctuations within the moving interface [10]. Note that β cannot be larger than 1/2 in NVG in particular and during spontaneous imbibition in general since otherwise the width would grow faster than than the height, which follows the Lucas-Wasburn law with exponent 1/2.

To investigate height fluctuations within the front [20] calculated the height-height correlation function:

$$C(\ell,t) = \langle (h(x,t) - h(x{+}\ell,t))^2 \rangle_{\mathrm{x}}^{1/2} \; . \tag{1}$$

The data shown in Fig. 2d exhibit neither scaling of $C(\ell,t)$ with ℓ nor any indication of spatial correlations in the experimentally accessible range 75 μm $\leq \ell \leq$ 4000 μm. Although the

correlations are reduced due to the projection in y-direction, the absence of any detectable correlation is in contrast to all previously reported experiments and theories on imbibition front roughening.

3. Scaling theory

The existing theories for spontaneous imbibition [3] are unable to reconcile the large roughness exponent and in particular the absence of lateral correlations. The latter could lead us to the conclusion that the porous space of Vycor glass could be represented by an ensemble of independent pores of random but constant radius as sketched in Fig. 3a. Such an ensemble of capillaries exhibits a roughening exponent 1/2 during spontaneous imbibition since the meniscus heights evolve independently from one another ($h_i(t) = a_i\sqrt{t}$ with random pre-factors a_i). However, this model is inappropriate for Vycor glass since pores have corrugated walls and therefore the pore radii vary strongly along individual pores, as sketched in Fig. 3b. Spontaneous imbibition in an ensemble of independent pores with radii which vary randomly along their length is described by a random deposition model, for which the roughness scales as $\sqrt{\langle h(t)\rangle}$, i.e with a roughening exponent 1/4.

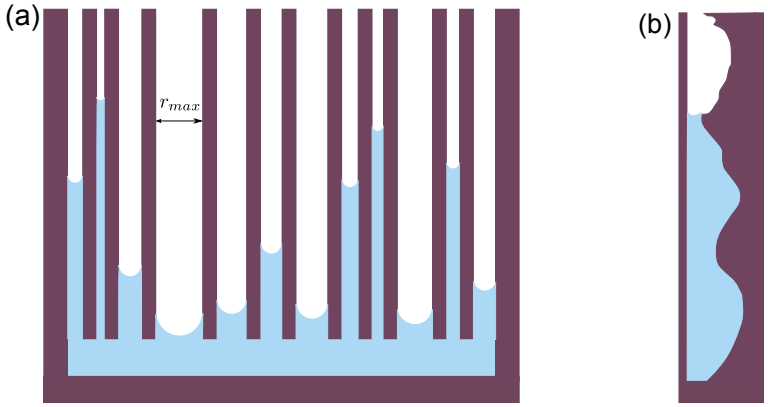

Figure 3. Sketch of independent pore models: (a) An ensemble of independent pores, each pore has a constant radius, radii of different pores vary randomly. During spontaneous imbibition the front width increases with $t^{1/2}$ (b) A pore with a corrugated wall, i.e. with a radius that varies along the pore axis. During spontaneous imbibition the front width increases with $t^{1/4}$.

For this reason independent pore models are inappropriate for NVG. Recently a lattice model for spontaneous imbibition in a silica aerogel predicted a roughening exponent $\beta \approx 1/2$. Silica aerogels have an extremely large porosity of 87–95 % which gives rise to a continuous liquid-gas interface. Consequently one expects here an effective surface tension to be present, inducing height-height correlations in the advancing imbibition front. The model details are thus also not appropriate for NVG, which must involve pore and network aspects.

With this background we proposed in [22] a scaling theory for spontaneous imbibition in porous media consisting of a network of interconnected elongated pores (Fig. 4). It is based on the observation that at pore junctions the meniscus propagation in the branch with the larger radius can come to a halt when the Laplace pressure of the meniscus exceeds the hydrostatic pressure within the junction. This leads to the emergence of voids behind the invasion front and concomitantly to anomalously fast front broadening as observed experimentally in NVG [20].

We consider a network of elongated pores with a length-to-width ratio of the order of 10, i.e. elongated, cylinder-like pores with random radii interconnected at pore junctions as sketched in Fig. 4. The bottom pores are connected to a liquid reservoir with pressure $P = 0$. We

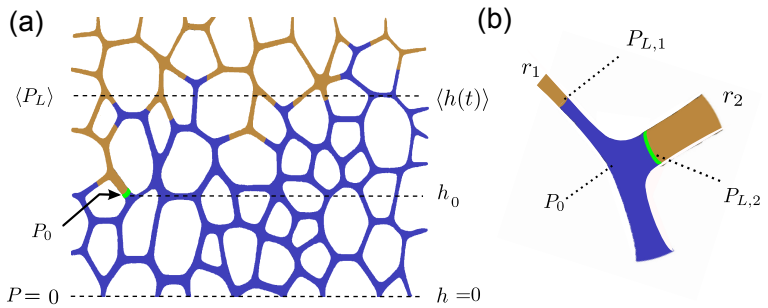

Figure 4. Sketch of a pore network with elongated pores (a) and an individual junction (b): r_i and $P_{L,i}$ denote the radius and Laplace pressure, respectively, in pore i, and p_0 denotes the hydrostatic pressure in the junction. In (b) $\langle h(t) \rangle$ and $\langle P_L \rangle$ denote the average height at time t and the average Laplace pressure.

assume that in each pore a liquid-gas interface forms, denoted as meniscus, that gives rise to a Laplace-pressure $P_L = -2\sigma/r$, where σ is the surface tension of the liquid and r the pore radius. If the pore radii vary between $r_{\min}$ and $r_{\max}$, the average radius is denoted by $\langle r \rangle$. Then, on large scales, the average height is expected to vary as $d/dt\, \langle h(t) \rangle = -\langle P_L \rangle / \langle h(t) \rangle$, which implies the Lucas-Washburn law $\langle h(t) \rangle \propto t^{1/2}$.

Consider now a junction at height h_0, where a pore branches into two (see Fig.4a). One branch has radius r_1, the other $r_2 > r_1$, yielding the Laplace pressures $P_{L,i} = -2\sigma/r_i$. Let P_0 be the hydrostatic pressure within the junction. As long as $P_{L,2} > P_0$ the meniscus in branch 2 is arrested. In the following we will answer the question how long the meniscus in branch 2 will be arrested and we will implicitly assume that it does not get annihilated by the filling of the pore from its other end. This means that we assume the radius r_2 also to be larger than the radius of the other branch of the junction of the other end. This reduces only the probability of this event by a r_2-dependent factor.

$P_0 = P_0(t)$ is a function of time and depends on how far the front has propagated and can be estimated as follows: Let the average front height be $\langle h(t) \rangle$. On average one expects the bulk pressure to decrease linearly from bottom to top:

$$P(\langle h(t) \rangle)/P_0 = \langle h(t) \rangle / h_0 \tag{2}$$

Therefore, with $P(\langle h(t) \rangle) = \langle P_L \rangle = -2\sigma \langle 1/r \rangle$ the average Laplace pressure, one obtains $P_0 = -2\sigma \langle 1/r \rangle \cdot h_0 / \langle h(t) \rangle$ and the condition $P_0 = P_{L,2}$ for the arrested meniscus to resume propagation (at time t_{resume}) reads

$$\langle h(t_{\text{resume}}) \rangle = h_0 r_2 \langle 1/r \rangle \; . \tag{3}$$

This equation has far reaching consequences:
1) The larger r_2 the longer the meniscus is arrested, and the average height that the front has to reach before the meniscus resumes propagation is proportional to the height where it stopped with a proportionality constant larger than one.
2) The time τ for which the meniscus is arrested is proportional to the time t_{stop}, when it stopped

$$\tau \propto t_{\text{stop}} \; . \tag{4}$$

To see this we note that with (3) one has $\langle h(t_{\text{stop}} + \tau) \rangle = h(t_{\text{stop}}) r_2 \langle 1/r \rangle$. With Lucas-Washburn $\langle h(t_{\text{stop}} + \tau) \rangle \propto (t_{\text{stop}} + \tau)^{1/2}$ and assuming that $h(t_{\text{stop}}) \propto t_{\text{stop}}^{1/2}$, too, for the relation between the height and the time when the considered meniscus stopped, one obtains (4).
3) Consequently from (4)

$$\tau \propto h^2(t_{\text{stop}}) = h_0^2; , \tag{5}$$

which implies that the probability distribution of arrest times for menisci arrested at height h will scale as

$$p_h(\tau) = h^{-2}\,\tilde{p}(\tau/h^2)\ . \tag{6}$$

4) The height difference $w_0(t_{\rm resume}) = \langle h(t_{\rm resume})\rangle - h_0$ is a measure for the local width of the propagation front (at the lateral coordinates of the position of the arrested meniscus) at time $t_{\rm resume}$. The ratio of this local width and the average height is $\frac{w_0(t_{\rm resume})}{\langle h(t_{\rm resume})\rangle} = 1-(r_2\langle 1/r\rangle)^{-1}$, which is independent of the time $t_{\rm resume}$. Thus all arrested menisci will contribute a time independent amount to the ratio of the average width $w(t)$ and average height. Since the width cannot grow faster than $h(t)$ this implies

$$w(t)/\langle h(t)\rangle = \text{const.}\ , \tag{7}$$

implying $w(t) \propto t^{1/2}$, i.e. a roughening exponent $\beta = 1/2$. Note that the invasion front dynamics is now expected to be be completely determined by the meniscus arrests, which in turn depend exclusively on the pore radii distribution and the height dependent hydrostatic pressure. Consequently one expects no lateral correlations in the meniscus heights to emerge, as observed in [20].

4. Microscopic model - computer simulations

The scaling theory presented in the last section neglects all geometric and topological details of a pore network. To test its predictions, we analyzed in [20, 22] the following microscopic model for spontaneous imbibition in a pore network with elongated pores [24, 23]: A two-dimensional square lattice of cylindrical capillaries inclined at 45° is considered, which consists of N_x and N_z nodes in horizontal and vertical directions, respectively. Capillaries, interconnected at nodes, have the same length L and random radii uniformly distributed over $[r_{\rm av} - \delta, r_{\rm av} + \delta]$. The average aspect ratio $2r_{\rm av}/L$ is set to 5. The pressure at the bottom nodes attached to the liquid reservoir is set to zero, the pressure at a moving meniscus is the Laplace pressure. Here we neglect gravity, which is justified as long as capillary forces are much larger than gravitational forces $2\sigma/r \gg \rho N_z L$, where ρ the specific weight of the liquid. This is the case for instance in experiments with NVG [21].

The dynamical evolution of the meniscus positions is driven by the hydrostatic pressures at the network nodes, which themselves depend on the meniscus positions. The node pressures P_i are determined by the boundary conditions plus the conservation of volume flux at each node: $\sum_j Q_{ij} = 0$, with Q_{ij} the volume flux from node i into the capillary j attached to it. According to Hagen-Poiseuille's Law $Q_{ij} = -c_{ij}\,\Delta P_{ij}/h_{ij}$, with $c_{ij}{=}\pi r_{ij}^4/8\eta$ and $\Delta P_{ij}{=}P_i{-}P_{L,ij}$. Here, r_{ij}, h_{ij} and $P_{L,ij}$ are the radius, the length and the Laplace pressure of the meniscus in capillary j attached to node i, respectively, and η is the viscosity of the liquid. The numerically calculated values for P_i and Q_{ij} are then inserted into the equation of motion for the heights given by $Q_{ij}{=}\pi r_{ij}^2\,dh_{ij}/dt$, which is then numerically integrated with an implicit Euler scheme with variable time step.

When a meniscus reaches the end of a capillary it immediately moves an infinitesimal distance $\delta{\simeq}0.01L$ into the adjacent capillaries, creating new menisci, as shown in Fig. 5a. When two menisci meet, they vanish, thus the capillary is entirely filled. If, due to a negative pressure difference, a meniscus retracts, it proceeds backward as long as its distance from the back node is larger than δ [see Fig. 5b]. When it reaches δ, the meniscus is stuck there until the driving pressure difference is again positive.

Fig. 5c shows a series of snapshots of the dynamical evolution of the meniscus positions and the filled pore area obtained from for a specific realization of random pore radii. The average front height $h(t) = \langle h_i(t)\rangle$ and average front width $w(t) = \langle (h_i(t) - h(t))^2\rangle^{1/2}$ are obtained by averaging over all meniscus heights h_i at time t and over different disorder (radii) realizations ($N = 100$). The result is shown in Fig.5d-f: We find that the average front height obeys the

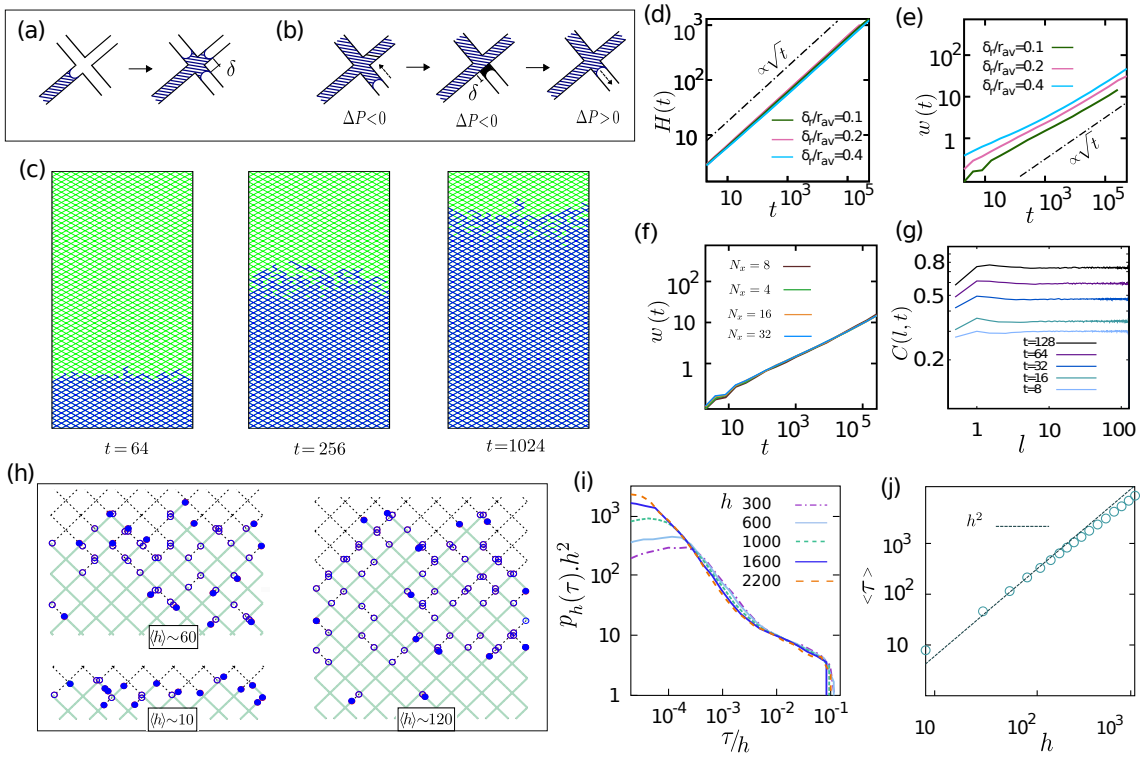

Figure 5. Micsocopic pore network model: a) After reaching an empty node, the liquid immediately fills the connected capillaries for a distance δ. b) After retracting up to δ toward a filled node, the meniscus is arrested until the pressure difference driving the liquid is again positive. c) Snapshots of meniscus configurations in a system with radius disorder strength $\delta r/\langle r\rangle = 0.3$ and lattice size 16×1000 at three different times (as indicated in units of nanoseconds). d) Evolution of the average front height $H(t)$ in a log-log plot for different radius disorder strengths $\delta r/\langle r\rangle$. The broken line indicates the Lucas-Washburn law $H(t) \propto t^{1/2}$. e) $w(t)$ for different radius disorder strengths $\delta r/\langle r\rangle$ for a pore network with $N_x = 16$ in a log-log plot. The broken line indicates the time dependence $w(t) \propto t^{1/2}$ predicted by the scaling theory described in section 3. f) Evolution of the front width $w(t)$ for different lateral system sizes N_x with $\delta r/\langle r\rangle = 0.1$ in a log-log plot. g) Height-height correlation function $C(l,t)$ as a function of the distance l at different times t (as indicated) for a sample with $\delta r/\langle r\rangle = 0.1$ and lattice size 128×32. h) Snapshots of the arrested (empty circles) and advancing (filled circles) menisci in the invasion front at three different times in a pore-network. Broken (full) lines represent empty (full) pores, $\langle h\rangle$ is the average height at the corresponding time. The filled circles represent moving menisci, the open circles indicate arrested menisci. i) Scaling plot of the meniscus arrest time distribution $P_h(\tau)$ according to Eq. 6. $\delta r/\langle r\rangle = 0.1$ and $N_x = 8$. j) Average meniscus arrest time $\langle\tau\rangle$ at a given height h for $\delta r/\langle r\rangle = 0.1$ and $N_x = 8$ in a log-log plot. The dashed line is proportional to h^2.

Lucas-Washburn $\sqrt{t}$-behavior (Fig. 5d) and that the width increases rapidly as $w(t) \propto t^{\beta}$ with β close to 1/2 (Fig. 5e), consistent with the scaling prediction eq.(7).

Remarkably the time evolution of the average width does not display any dependence on the lateral system size, as seen in Fig. 5f. The absence of finite size effects is an indicator of a small or vanishing correlation length scale for height-height fluctuations. Within the framework of the scaling theory of roughening [25, 26], the interface width in a finite system of lateral size N_x is expected to grow algebraically $w(t) \sim t^{\beta}$ as long as the system size is larger than the correlation length, $\xi(t)/L \ll N_x$, and only saturates to a constant $w(t) \approx$ const. as soon as the correlation length exceeds the system $\xi(t)/L \gg N_x$. Since the data in Fig. 5f display an algebraic growth even for the smallest system size $N_x = 4$ the correlation length must be smaller than $4L$. This is confirmed by the height-height correlation function $C(\ell, t)$ (eq. 1, Fig. 5g), which saturates

quickly (around $\ell \approx L$). Scaling theory [25, 26] predicts saturation of $C(\ell, t)$ for $\ell \gg \xi(t)$, which implies $\xi(t)/L = \mathcal{O}(1)$ independent of time t. This finding is also in agreement with the experimental result for $C(\ell, t)$ in NVG (Fig. 2d).

Our scaling theory presented in the last section explains the origin of the large roughness exponent $\beta = 1/2$ and the absence of lateral height-height correlations, namely long lasting meniscus arrests with arrest times that are of the same order as the the time when the arrest started. Fig. 5h shows snapshots of arrested and moving menisci in our model and one sees that with progressing time most menisci are actually arrested and only a few move. We analyzed the probability distribution of the arrest times $P(\tau)$ in our model [22] and found that indeed the intermediate and large time regime of the distribution, including the cut-off, scale nicely with h^2 as predicted by Eq.(6), as is shown in Fig. 5i. Consequently the average arrest time $\langle\tau\rangle$ grows with time as $h^2(t)$ as shown in Fig.5j.

The invasion front thus involves a finite fraction of the occupied volume and comprises connected clusters of empty pores whose size distribution gets broader with increasing time. Based on the conditions for meniscus arrests presented above one can derive a scaling form for the distribution of (void) cluster sizes [22].

5. Meniscus arrest in asymmetric pore junctions

The basic assumption of the scaling theory for spontaneous imbibition in porous media with elongated pores described in section 3 as well as the microscopic pore model presented in section 4 are long-lasting meniscus arrests in asymmetric pore junctions. Since such meniscus arrests have not been studied quantitatively before, we investigated in [27] the capillary rise of a fluid in a Y-shaped junction of channels with different radii experimentally and theoretically. We consider here a channel junction geometry as sketched in Fig. 6a, with cylindrical channels of radius r_f for the feeding channel that is connected to the liquid reservoir, and radius r_n and r_w for the narrow and wide branch, respectively. A simplified model for the capillary rise in this asymmetric Y-junction predicts that once the meniscus reaches the junction and splits into two menisci, the meniscus in the wide branch proceeds to propagate whereas the meniscus in the narrow channel is arrested until the meniscus in the wide channel reaches the distance $l_{\rm resume}$ from the junction, which is proportional to l_0, the length of the feeding channel and given by [27]:

$$l_{\rm resume} = l_0 \cdot \alpha \quad \text{with} \qquad \alpha = \frac{c_n}{c_f}\left(\frac{P_{L,n}}{P_{L,w}} - 1\right) . \tag{8}$$

Here $P_{L,i} = 2\sigma\cos\theta/r_i$ is the Laplace pressure (the index $i \in \{f, n, w\}$ refers to the feeding, narrow and wide channel, respectively) and σ the surface tension, $c_i = \pi r_i^4/8\eta$ with η the viscosity of the liquid. For channels with rectangular cross section the expressions for $P_{r,i}$ and c_i have to be replaced by expressions involving the widths and the heights of the channels.

The arrest time is the time that the meniscus in the wide channel needs to reach the distance $l_{\rm resume}$ from the junction and is is proportional to l_0^2 and given by [27]:

$$\tau = K \cdot l_0^2, \quad \text{with} \qquad K = \frac{A}{|P_{L,n}|}\frac{c_n}{c_f^2} \cdot \left\{ \left(\frac{P_{L,n}}{P_{L,w}} - 1\right) + \frac{1}{2}\left(\frac{P_{L,n}}{P_{L,w}} - 1\right)^2 - \frac{c_f}{c_n} - \frac{c_f^2}{2c_n^2} \right\} . \tag{9}$$

Here A is the cross sectional area of the channel $A = \pi r^2$.

The equation (8) is equivalent to the eq.(3) occurring in the scaling theory presented in section 3. In [27] we used an experimental, microfluidic setup to demonstrate the validity of eq.(8), and concomitantly a basic ingredient of the scaling theory, eq.(3). Experimental results for capillary rise in an asymmteric Y-junction are shown in Fig. 6b, which shows a series of snapshots of the rising liquid and arrested meniscus in the microfluidic device, and Fig. 6c,

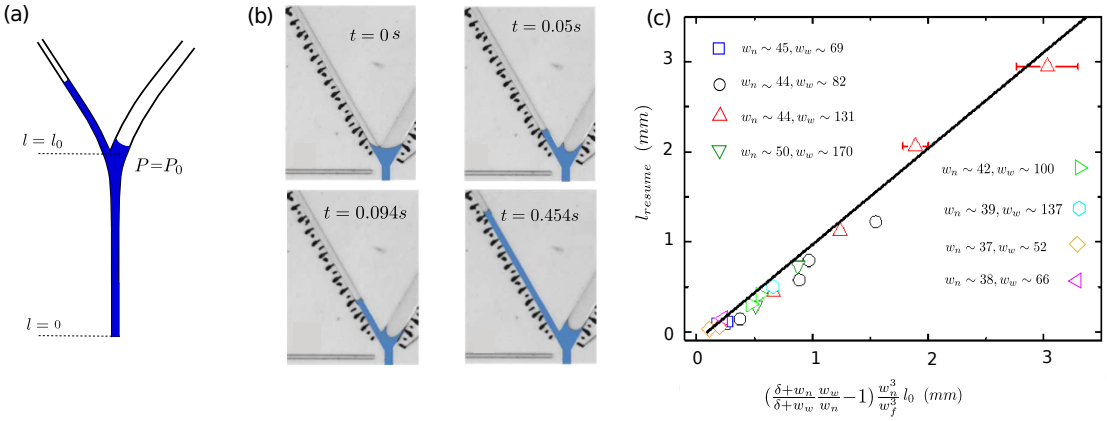

Figure 6. Capillary rise in asymmetric pore junctions – microfluidic experiments: (a) Schematic shape of a Y-junction. (b) Time series of fluorinated oil FC-70 invading a microfluidic Y-junction with a long feeding channel demonstrating the arrest of the meniscus in the wide channel during the initial propagation of the meniscus in the narrow channel. The dimensions of the device are $w_n \sim 45\mu m$, $w_w \sim 131\mu m$ and $l_0 = 8800 \pm 120\mu m$. (c) Experimental result for $l_{\rm resume}$, as a function of the rescaled length of the feeding channel l_0, for different junction geometries (from [27]). The values of w_n and w_w of each device are indicated in μm. The line displays the theoretical prediction. Error bars in x- and y-direction are omitted if there are smaller than the symbol size.

which shows the experimentally measured arrest time τ as a function of the scaled variable $l_{\rm resume} = l_0 \cdot \left(\frac{\delta+w_n}{\delta+w_w} \cdot \frac{w_w}{w_n} - 1\right) \cdot \frac{w_n^3}{w_f^3}$. Indeed the data points from different experiments (different feeding channel lengths, different channel widths) lie on a straight line as predicted by eq.(3).

Thus we have experimental evidence for the meniscus arrests and its duration in asymmetric pore junction as they occur in random pore networks, which supports the basis of the scaling theory of section 3. The simplified model for capillary rise as sketched above is based on macroscopic laws (Laplace pressure, Hagen-Poisseuille), which are indeed expected to hold for the experimental microfluidic device used to validate the model predictions. The question remains, whether meniscus arrests together with the scaling relations for arrest time etc. can also be observed on the nanometer scale, which is the appropriate length scale for the experiments on NVG described in section 2.

Experimentally it is not yet feasible to explore meniscus arrest on the nano-scale, but molecular dynamics simulations are very well suited for studying physical processes on this length scale. Therefore we considered a capillary junction formed by silica walls attached to a reservoir of argon molecules and performed molecular dynamics simulations of the capillary rise [28]. Snapshots of the particle configurations at different times are shown in Fig. 7. As it can be seen, the meniscus in the wide channel is indeed arrested for a time that is of the same order of magnitude as the time the meniscus in the feeding channel needed to reach the junction. A quantitative analysis necessitates many of these runs to obtain good statistics and is under way.

6. Discussion

We have shown that the dynamics of spontaneous imbibition in nanoporous media with elongated pores (low porosity), like NVG, is dominated by long-lasting mensicus arrests in the wide channels at pore junctions of channels with different radii. This establishes a new universality class for imbibition front roughening, which is actually predicted to be independent of the dimensionality of the pore network and mainly dependent on the pore radius distribution. The independence of dimensionality and topology of the pore network is expected due to a lack of

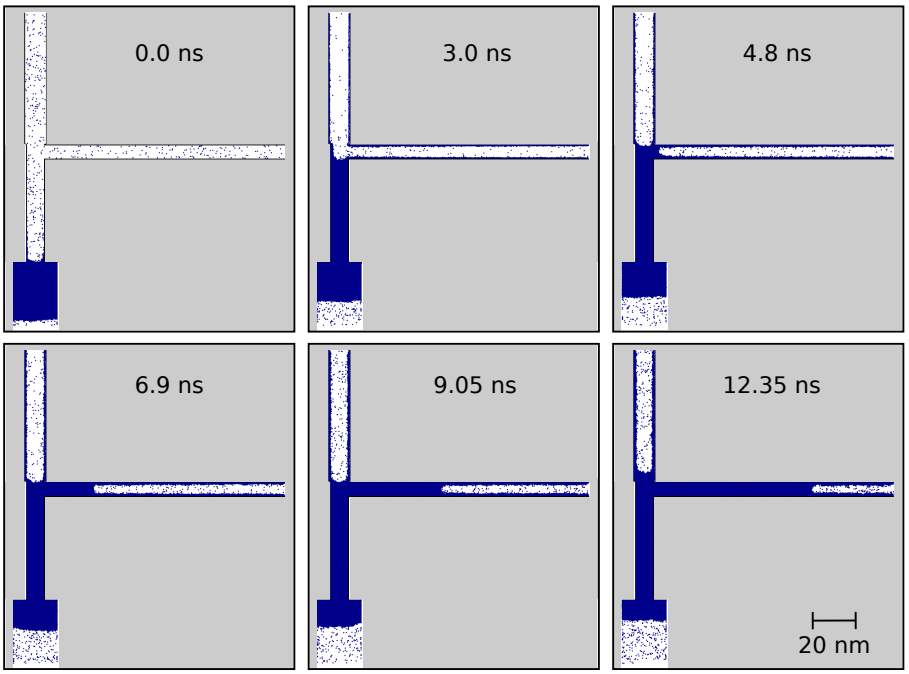

Figure 7. Capillary rise in asymmetric pore junctions – molecular dynamics simulation: Six snapshots from the molecular dynamics simulations of the spontaneous imbibition of liquid argon in silica nano-pores are taken at consecutive timesteps. The nano-pore consists of 98,540 silica atoms in three channels. The feeding channel has a diameter of 4.0 nm, the upper channel 4.8 nm and the right channel 3.2 nm. The interactions between the 191,012 argon atoms are given by a Lennard-Jones potential with the parameters $\epsilon = 0.2384 \frac{\text{kcal}}{\text{mole}}$ and $\sigma = 3.4\mathring{A}$. The potential is cut off at a distance of $10.0\mathring{A}$. Temperature is kept at a constant value of 94 K with the help of the DPD-thermostat. The parameters of the Lennard-Jones interactions between the wall and the argon atoms are $\epsilon = 0.1521 \frac{\text{kcal}}{\text{mole}}$ and $\sigma = 3.85\mathring{A}$. After filling the feeding channel the liquid penetrates the narrow channel and the rise of the meniscus is stopped for about 4.46 ns in the wide channel.

spatial correlation between the individual meniscus arrests. This meniscus arrest universality class should also be valid for forced imbibition in pore networks with elongated pores as long as the reservoir pressure is much smaller than the modulus of the Laplace pressures in the network. For applications it is interesting to note that the dependence of the imbibition front broadening on the pore radius distribution might be utilized to infer from the meniscus arrest time distribution or characteristics of the front broadening process dependent upon it back onto the radius distribution.

For decreasing aspect ratio (ratio of pore radius over pore length) one expects at some point a continuous liquid-gas interface to form and thus a crossover from the meniscus arrest universality class to a different universality class, where the liquid-gas-interface surface tension becomes relevant. In [29] we studied a model which was devised to capture some of the physics relevant for this crossover. It predicts that for non-vanishing effective surface tension the propagation of the imbibition front comes to a halt at some point.

Nanoporous materials become more and more important in fundamental research and nanotechnology [30]. Recently [31] it was shown that for aqueous electrolyte imbibition in nanoporous gold the fluid flow can be reversibly switched on and off through electric potential control of the solidliquid interfacial tension, which implies that one could accelerate the imbibition front, stop it, and have it proceed at will. In this respect it would be rewarding to generalize our scaling theory for the arrest time distribution and front broadening to field or time dependent Laplace pressures and to have a closer look with our microscopic pore network

model into the imbibition dynamics in this new class of nanoporous materials.

Acknowledgments
We thank P. Huber, D.-S. Lee, M. Jung, and R. Seemann for fruitful collaborations and stimulating discussions. We acknowledge financial support from the German Research Foundation under Grant No GRK 1276.

References

[1] Bear J 1972 *Dynamics of Fluids in Porous Media* (New York: Elsevier)
[2] Sahimi M 1993 *Rev. Mod. Phys.* **65** 1393
[3] Alava M, Dube M and Rost M 2004 *Adv. Phys.* **53** 83
[4] Todd D K and Mays L W 2005 *Groundwater Hydrology* (John Wiley)
[5] Geromichalos D, Mugele F and Herminghaus S 2002 *Phys. Rev. Lett.* **89** 104503
[6] Buldyrev S V, Barabási A L, Caserta F, Havlin S, Stanley H E and Vicsek T 1992 *Phys. Rev.* A **45** R8313
[7] Horváth V K and Stanley H E 1995 *Phys. Rev.* E **52** 5166
[8] Hernandez-Machado A, Soriano J, Lacasta A M, Rodríguez M A, Ramírez-Piscina L and Ortín J 2001 *Europhys. Lett.* **55** 194
[9] Planet R, Pradas M, Hernandez-Machado A and Ortin J 2007 *Phys. Rev.* E **76** 056312
[10] Dubé M, Daneault C, Vuorinen V, Alava M and Rost M 2007 *Eur. Phys. J.* B **56** 15
[11] Lucas R 1918 *Kolloid* Z **23** 15
[12] Washburn E W 1921 *Phys. Rev.* **17** 273
[13] Dimitrov D I, Milchev A and Binder K 2007 *Phys. Rev. Lett.* **99** 054501
[14] Gruener S, Hofmann T, Wallacher D, Kityk A V and Huber P 2009 *Phys. Rev.* E **79** 067301
[15] Reyssat M, Courbin L, Reyssat E and Stone H A 2008 *J. Fluid Mech.* **615** 335
[16] Dullien F A L 1992 *Porous Media, Fluid Transport and Pore Structure* (San Diego: Academic Press)
[17] Dube M, Rost M and Alava M 2000 *Eur. Phys. J* B **15** 691
[18] Gelb L D, Gubbins K E 1998 *Langmuir 1998* **14** 2097
[19] Song Y Q, Ryu S, Sen P N 2000 *Nature* **406** 178
[20] Gruener S, Sadjadi Z, Hermes H E, Kityk A V, Knorr K, Egelhaaf S U, Rieger H, and Huber P 2012 *Proc. Nat. Acad. Sci. USA* **109** 10245
[21] Caupin F, Cole M W, Balibar S and Treiner J 2008 *Europhys. Lett.* **82** 56004
[22] Sadjadi Z and Rieger H 2013 *Phys. Rev. Lett.* **110** 144502
[23] Aker E, Maloy K J, Hansen A, and Batrouni G G 1998 *Transp. Porous. Med.* **32** 163
[24] Lam C H and Horvath V K 2000 *Phys. Rev. Lett.* **85** 1238
[25] Barabasi A L and Stanley H E 1995 *Fractal Concepts in Surface Growth* (New York: Cambridge University Press)
[26] Krug J 1997 *Adv. Phys.* **46** 139
[27] Sadjadi Z, Jung M, Seemann R, and Rieger H 2015 *Langmuir* **31** 2600
[28] Plimpton S 1995 *J. Comp. Phys* **117** 1, http://lammps.sandia.gov
[29] Lee D K, Sadjadi Z, and Rieger H 2014 *Phys. Rev. E* **90** 013016
[30] Huber P 2015 *J. Phys. Condens. Matter* **27** 103102
[31] Xue Y, Markmann J, Duan H, Weissmüller J and Huber P 2014 *Nature Comm.* **5** 4237